

Chapter 14

Bovine Serum Albumin 3D Structure Determination by THz Spectroscopy and Molecular Modeling

Maria Mernea, Aurel Leca, Traian Dascalu, Dan Mihailescu

Abstract The low frequency collective movements of proteins associated with biologically relevant conformational transitions are situated in the terahertz (THz) spectral region. THz spectroscopy experiments have revealed that each molecular species has a unique absorption pattern in THz domain. We used time-domain THz spectroscopy (TDS) to study the conformation and flexibility of bovine serum albumin (BSA), a protein whose 3D structure is unknown. We performed THz spectroscopy experiments on lyophilized BSA. Theoretical spectra were obtained by normal modes analysis performed on BSA structures generated by homology modeling and molecular dynamics simulations. The agreement between experimental and theoretical data allowed us to validate the model of BSA and also to gain insight into BSA vibrations in THz domain.

14.1 Introduction

Protein structure and flexibility knowledge is crucial for understanding protein function at the molecular level. Low frequency collective movements of proteins associated with biologically relevant conformational transitions are situated in the

Maria Mernea

Faculty of Biology, University of Bucharest, Bucharest, 050095, Romania,
e-mail: maria.merneanu@bio.unibuc.ro

Aurel Leca

National Institute for Laser, Plasma and Radiation Physics, Laboratory of Solid-State Quantum Electronics, Bucharest R-077125, Romania, e-mail: aurel.leca@inflpr.ro

Traian Dascalu

National Institute for Laser, Plasma and Radiation Physics, Laboratory of Solid-State Quantum Electronics, Bucharest R-077125, Romania, e-mail: traian.dascalu@inflpr.ro

Dan Mihailescu

Faculty of Biology, University of Bucharest, Bucharest, 050095, Romania,
e-mail: dan.mihailescu@bio.unibuc.ro

terahertz (THz) spectral region [8]. Therefore, Time-domain spectroscopy (TDS) became a promising technology for protein structure and conformational changes investigation.

Bovine serum albumin (BSA), is a globular protein found in bovine plasma. It's 3D structure is yet unknown. In a previous study, we built a 3D model of BSA based on the homology with human serum albumin. Based on the model, we generated several other possible BSA conformations by molecular dynamics and simulated annealing molecular dynamics simulations. Only one model was validated based on the agreement between theoretically derived THz spectra of the BSA structures and the experimentally derived spectrum [6].

We present here the experimentally derived THz spectrum of BSA against the simulated THz spectrum based on our 3D model of BSA. The observed THz absorption of BSA is explained based on the results of normal modes analysis.

14.2 THz Experiments

In our THz-TDS experiments, we used a 780 nm wavelength, 80 mW average power and 150 femtosecond (fs) pulse length self mode locked fiber laser that emits a fs optical pulse train with a repetition rate of 90 MHz. The optical pulse train is divided in two equivalent beams by a beam splitter and are used to irradiate the photoconductive antenna and to gate the photoconductive receiver. The THz source is represented by a DC biased microstrip photoconductive antenna fabricated on low-temperature grown GaAs (LT-GaAs) 400 μm thick substrate. After encountering the THz source, the first beam is focused by an integrated silicon lens between the electrodes. When conductivity changes in semiconductor are induced by the optical excitation, THz pulses are produced. The maximum bias voltage is 80 V and the emitted average power of THz radiation is 10 μW . The THz pulse is focused using polyethylene lens onto the sample. The beam emerging from the sample is expanded by another polyethylene lens and directed onto the THz detector. The detector has a similar structure as the emitter and works as an unbiased antenna. The photo-conductive gap of the antenna is gated by the ultra short optical pulses of the second beam provided by the beam splitter. The THz pulse provides the bias voltage pulse accelerating the charge carriers to create a current that is amplified and recorded. Pulses synchronization is assured by the delay line based on a hollow retro reflector placed in the pumping beam path. By scanning the optical delay line in 10–20 fs steps, the waveform of electric field of THz radiation is build. The signal of the THz detector is pre-amplified and detected by a lock-in amplifier using a 50 kHz reference frequency to modulate the emitter bias voltage. The Fourier transform of waveform gives the spectral content of THz radiation.

The biological sample that we analysed was a 0.5 mm thick layer of lyophilised BSA. The sample was placed in a teflon holder. We recorded THz spectra with and without the sample inserted into the THz beam path. The THz absorption spectrum of BSA is derived from the comparison between these. In order to improve

the accuracy of THz measurements, random noise and systematic errors were suppressed by averaging multiple complex spectra (equivalent with time pulses averaging). We recorded spectral information about lyophilized BSA up to 2.8 THz with a spectral resolution of 7.4 GHz. The methods used for data processing are described in detail elsewhere [3].

14.3 Theoretical Methods

We calculated the theoretical THz spectra of BSA using normal modes analysis (NMA) [7] performed with CHARMM [2]. THz vibration frequencies of BSA were obtained from the normal mode eigenvalues of the mass-weighted Hessian. The intensities of each normal mode were calculated from the dipole derivatives as given by the equation [5]:

$$I_i = \left[\sum_{j=1}^{3N} \frac{\partial \mu_j}{\partial r_j} X_{ij} \right]^2 \quad (14.1)$$

where the sum is over all $3N$ coordinates, $\frac{\partial \mu_j}{\partial r_j}$ represents the dipole moment and X_{ij} represents the corresponding eigenvectors derived from the diagonalization of the mass-weighted Hessian. THz spectra were calculated using a Lorenzian function to describe each intensity line, as given by:

$$I(v_j) = \frac{I_{max} \Gamma^2}{\pi [(v - v_i)^2 + \Gamma^2]} \quad (14.2)$$

The lines were uniformly broadened to a temperature of 300 K and the Γ value (window width parameter) was set 0.6 THz, the value given by the experimental setup.

The electrostatic surface potential of the BSA model was calculated using the Adaptive Poisson Boltzmann Solver (APBS) software [1] through APBS electrostatics extension of VMD [4], using the default settings in APBS.

14.4 Results

Through NMA performed on BSA, we generated 1994 vibration modes for the BSA model of vibrations up to 4.03 THz. The simulated THz spectrum of dry BSA against the experimental spectrum is presented in Fig. 14.1(a). In order to compare experimental and theoretical data, we took into account the low-frequency range of 0.3–1 THz. For this frequency range, we determined the slopes of the lines that fit the spectra. The slope of the line that fits the theoretical spectrum is 13.56 ± 0.3 and has a close value to the slope of the line that fits the experimental spectrum, that has a value of 13.8 ± 0.25 . Still, the theoretical spectrum was calculated using the window

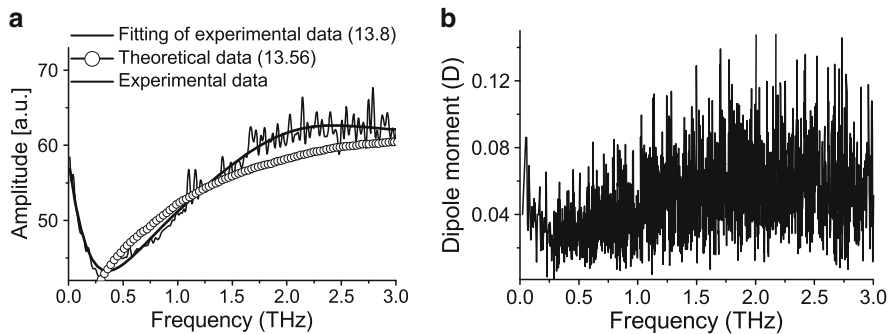


Fig. 14.1 Experimental and simulated THz spectra of dry BSA. The slope of the lines that fit these spectra in the 0.3–1 THz frequency range are labelled between brackets (a) and total dipole moment plotted against the frequency of vibrations for dry BSA. The dipole moment is measured in debye (D); 1 D = $3.33564 \times 10^{-30} C \times m$ (b)

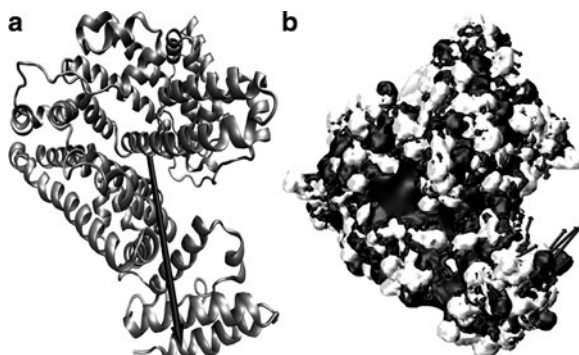


Fig. 14.2 The 3D model of BSA. The dipole moment of BSA is represented with a black vector with the direction from net negative charge to net positive charge (a) and The amplitude and directions of BSA C-alpha atoms displacements during the lowest non-zero frequency mode are represented with black vectors. For the electrostatic potential surface we used white to represent the negative areas and black to mark positive areas (b)

width parameter value given by our experimental setup ($\Gamma = 0.6$ THz). For this Γ value, THz absorptions are represented by their average over all frequencies and hide any distinct spectral features. Since the THz absorption depends on the fluctuations of the protein dipole moment, we investigated this aspect on BSA. Total dipole moment plotted against the frequency of vibrations is presented in Fig. 14.1(b). As seen in Fig. 14.1, the dipole moment fluctuations calculated through NMA strongly resemble the absorption spectrum derived by experiment, even for frequencies below 0.3 THz or above 1 THz. In Fig. 14.2(a) we present the total dipole moment vector calculated for BSA. BSA comprises 579 residues, from which 98 are negatively charged, while 81 are positively charged. These residues are scattered throughout the structure and contribute to the total dipole moment of BSA. For instance, the

vectors corresponding to BSA C-alpha atoms displacements during the lowest non-zero frequency mode and the disposition of electrostatic potential on the surface of BSA are presented in Fig. 14.2(b).

14.5 Discussion

The knowledge provided by THz spectroscopy can be supplemented by information provided by molecular modeling. Since the crystal structure of BSA is unknown, we simulated BSA THz spectra using a 3D model of BSA and we obtained a good agreement with the experiment. The correlation is reflected by the similar values of the lines that fit experimental and theoretical spectra up to 1 THz, and also by the calculated protein dipole moments fluctuations that are in agreement with the experiment for up to 3 THz. THz spectroscopy assisted by molecular modelling is a promising approach for protein 3D structures determination.

Acknowledgement The research presented here was funded by MEC-ANCS 62-055/2008 grant.

References

- [1] Baker, N.A., Sept, D., Joseph, S., Holst, M.J., McCammon, J.A.: Electrostatics of nanosystems: application to microtubules and the ribosome. *Proc Natl Acad Sci U S A* 98(18), 10037-10041 (2001).
- [2] Brooks B. R., Olafson B. D., Swaminathan S., and Karplus M.: CHARMM: A Program for Macromolecular Energy, Minimization, and Dynamics Calculations. *J. Comp. Chem.* 4, 187-217 (1983).
- [3] Dinca, M.P., Leca, A., Apostol, D., Mernea, M., Calborean, O., Mihailescu, D., Dascalu, T.: Transmission THz Time Domain System for Biomolecules Spectroscopy. *Journal of Optoelectronics and Advanced Materials* 12(1), 110-114 (2010).
- [4] Humphrey, W., Dalke, A., Schulten, K.: VMD: visual molecular dynamics. *J Mol Graph* 14(1), 33-38, 27-38 (1996).
- [5] Jaaskelainen, S., Verma, C.S., Hubbard, R.E., Linko, P., Caves, L.S.: Conformational change in the activation of lipase: an analysis in terms of low-frequency normal modes. *Protein Sci* 7(6), 1359-1367 (1998).
- [6] Mernea, M., Calborean, O., Dinca, M.P., Leca, A., Apostol, D., Dascalu, T., Mihailescu, D.: The Simulation of Bovine Serum Albumin Vibration Spectrum in THz Domain. *Journal of Optoelectronics and Advanced Materials* 12(1), 135-140 (2010).
- [7] Tama, F., Gadea, F.X., Marques, O., Sanejouand, Y.H.: Building-block approach for determining low-frequency normal modes of macromolecules. *Proteins* 41(1), 1-7 (2000).
- [8] Tama, F., Sanejouand, Y.H.: Conformational change of proteins arising from normal mode calculations. *Protein Eng* 14(1), 1-6 (2001).